

'Perfect' Crystals in Crystal Structure Analysis

BY MICHAEL HART

Schuster Laboratory, Department of Physics, University of Manchester, Manchester M13 9PL, England

(Received 15 October 1994; accepted 4 January 1995)

Abstract

There is still a great deal to be learned by detailed studies of even the very simplest crystals about the foundations of X-ray diffraction. From the theoretical viewpoint there are two forms of 'perfect' crystals; the obvious case is that which is normally referred to as ideally perfect, exemplified by single crystal silicon, and the other less obvious form is the ideally imperfect sample which obeys precisely the kinematic theory of diffraction. Although such samples do not exist under normal laboratory X-ray conditions, at high X-ray energies real samples satisfy more and more closely the simple theory. With zero absorption and pure kinematic scattering becoming the norm at high energies, it seems possible that small structurally imperfect single crystals and even powdered samples could be used for sub-percentage measurements of structure factors. The necessary diffraction conditions are explored in this paper.

1. Introduction

Gamma-ray diffraction is a widely recognized but little practised technique which has been thoroughly and productively explored using radioactive sources. Following the first demonstration of gamma-ray Bragg reflection from crystals of rock salt by Rutherford & Andrade (1914) from radioactive radium sources, almost no studies of crystals were undertaken until the 1970s when sufficiently intense nuclear gamma-ray sources, activated by neutron irradiation in thermal reactors, became available (Freund, 1973; Schneider, 1980, 1981). Most of the early work was concerned with studies of micro- and macroscopic strain in single crystals and polycrystalline materials, making use of the penetrating power of the hard radiation to study bulk material and using large samples so as to increase the detected intensity.

Structural studies of single crystals were first made approximately 10 years ago. Graf & Schneider (1986) were the first to realise that structure factors can be measured with high precision in imperfect crystals because they effectively become *ideally* imperfect at high enough X-ray energies. At the other extreme, appropriate materials show *Pendellösung fringes* with high contrast, corresponding to almost zero absorption, at these energies (Alkire, Yelon & Schneider, 1982; Alkire & Yelon, 1981) so that accurate structure factors can be

determined. These experiments used nuclear gamma lines at 468.1, 316.5 and 103 keV.

Against this background, proposals were made to build high-energy beamlines at synchrotron radiation facilities (Freund, Hart & Schneider, 1988; Freund, 1988). Techniques are under development for high-energy X-ray measurements and the first synchrotron radiation experiments at 150 keV showed that multiple Bragg-reflection X-ray optics using channel-cut crystals can be conveniently used and that very high intensity and high signal-to-noise ratios can also be obtained (Hastings, Siddons, Berman & Schneider, 1989).

1.1. Proposed experimental regime

By working at a sufficiently high X-ray energy the advantages of low absorption, no extinction and reasonably large crystals, can all be realised. With high-intensity beams from insertion devices on high-energy storage rings, structure factors become measurable with very high precision, allowing detailed studies of static and dynamic charge densities.

2. Theoretical background

2.1. Dynamical theory

For the Laue case of transmission in a weakly absorbing perfect crystal, Zachariasen (1945) gives the reflectivity for a plane wave as

$$I_H/I_0 \approx \exp(-\mu t / \cos \theta) [\sin^2(A\{1+y^2\}^{1/2}/\{1+y^2\}) + \sinh^2(\kappa A/\{1+y^2\}^{1/2})/\{1+y^2\}]. \quad (1)$$

The unfamiliar symbols are defined as

$$A = \pi t / \Delta_0^\sigma \quad y = \Delta \theta \Delta_0^\sigma / d \quad \kappa = \chi_{lh} / \chi_{rh} \\ \Delta_0^\sigma = \lambda \cos \theta / \chi_{rh} \quad \Delta_0^\pi = \lambda \cos \theta / C \chi_{rh}.$$

χ_{lh} and χ_{rh} are defined in Pinsker (1978) and values are given on pp. 95 and 97, respectively. Values of κ (p. 137), Δ_0^σ (p. 54) and μ (p. 87) are also given there. For silicon and $\text{Ag}K\alpha_1$, p. 87 gives $\mu = 7.38 \text{ cm}^{-1}$ and for the 220 Bragg reflection $\chi_{rh} = 1.179 \times 10^{-6}$ and $\chi_{lh} = 0.00625 \times 10^{-6}$ (p. 97). For a crystal 100 μm thick, the absorption pre-factor in (1) is 0.929, the \sin^2 factor is of the order unity and, for $y = 0$, the \sinh^2 term

is 0.0016. This last term is therefore negligible for thin silicon at energies above 22 keV. The intensity is, then, to better than 1%, given by

$$I_H/I_0 \approx [\sin^2(A[1+y^2]^{1/2})/(1+y^2)], \quad (2)$$

where

$$A = e^2 \lambda [F_H F_{-H} C^2]^{1/2} t / mc^2 V [\gamma_0 \gamma_H]^{1/2}. \quad (3)$$

$C = 1$ for σ -case and $C = |\cos 2\theta|$ for π -case polarization. If we ignore the (small) changes in anomalous dispersion f' then $\Delta_0 \propto E \cos \theta / C$, so that the scaling relations are

$$y \propto E \cos \theta / C \quad \text{and} \quad A \propto C / E \cos \theta. \quad (4)$$

For low-order reflections at high energies $\cos \theta \approx 1$, so that both y and A^{-1} scale linearly with energy.

These examples show that at energies substantially higher than 22 keV the approximation of zero absorption is quite accurate. The corresponding integrated reflecting power is given by the following equations from Zachariassen's book, Z 3.165 and Z 3.167, as

$$R_L = (1/2)\pi \int_0^{2A} J_0(x) dx = \pi \sum_n J_{2n+1}(2A) \quad (5)$$

and $R_B = \pi \tanh A.$

Fig. 1 shows graphs of these two results. For $A < 0.8$ the two results are indistinguishable. Thus, the crystal diffraction geometry has no effect on the integrated reflectivity. The same result can be seen analytically, as Zachariassen shows, for both $\tanh A$ and $\sum_n J_{2n+1}(2A)$ are equal to A for $A \ll 1$. Absorption is negligible too so that single-crystal diffraction in that size regime is determined entirely by the sample volume rather than by geometrical factors related to absorption and refraction.

2.2. Kinematical theory

So far we have explored the dynamical region in the thin crystal, the low absorption limit which is appropriate

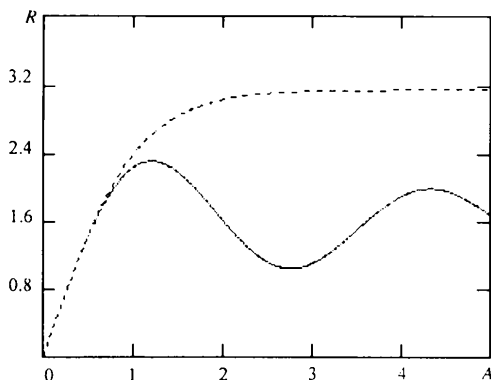


Fig. 1. Integrated intensity in terms of the parameter A ; $A = \pi$ corresponds to $t = \Delta_0$, see Table 1 for typical values. Upper curve is for the Bragg case, lower curve is for the Laue case.

to the high-energy diffraction regime. We now assemble the corresponding results within the kinematic, *single scattering*, theoretical approximation and will later seek to merge the two results in an exploration of the experimental opportunities presented by high-energy, bright synchrotron X-ray sources.

Microcrystal diffraction has been an area of intense activity in the last few years at synchrotron radiation facilities. However, the main thrust of the activity has been to explore the possibility of using tiny crystals, especially for materials of which large samples cannot be grown. The conclusion relevant to the present discussion is that samples as small as $1 \mu\text{m}$ in diameter do give observable intensities from existing synchrotron radiation sources and that the only important barriers to progress in the direction of using these and even smaller samples in diffraction experiments are the technical ones of sample handling and signal-to-noise ratio control. The following comments derive from a review by Rieck & Schulz (1991).

A convenient, although not necessarily correct, starting point for the diffracted intensity, I in photons s^{-1} , was given by Wölfel (1975)

$$I = (e^2/mc^2)^2 \{ [1 + \cos^2 2\theta] / [2 \sin 2\theta] \} \{ (F_{hkl}/V)^2 \lambda^3 V \} I_0. \quad (6)$$

Here, I_0 is the flux at the sample in photons $\text{s}^{-1} \text{mm}^{-2}$ and the first term is the single electron-scattering power. The term in $\{ \}$ is the Lorentz polarization factor, which need not concern us here, while the third term is simply the scattered intensity per unit cell expressed with the unit cell volume V , in units of the wavelength λ . A practical problem with this formulation is that it represents the integrated reflection power in a situation where the mosaic spread of the sample and its relationship to the divergence and energy spread of the incident beam is not necessarily clearly defined or straightforward.

The conclusion of the calculations, backed by experiments using second-generation storage ring sources, is that the Bragg scattering from a $1 \mu\text{m}^3$ sample should be measurable (*i.e.* should provide a counting rate of *ca* 1s^{-1}) with a present-day storage ring such as the ESRF [Rieck & Schulz (1991)]. It is important to remember that the X-ray scattered intensity from a $1 \mu\text{m}$ diameter X-ray beam by $1 \mu\text{m}$ of solid material is about the same as the scattered intensity from 1mm of air.

The kinematic theory results are valid up to a crystal thickness where absorption is significant or where double and multiple scattering must be taken into account.

2.3. X-ray absorption

At 40 keV the absorption coefficient for materials is less than *ca* $25 \text{cm}^2 \text{g}^{-1}$. Taking a typical density of 4g cm^{-3} gives an absorption length of *ca* $100 \mu\text{m}$. The highest value of the absorption coefficient is for those

elements which have K -edges at ca 40 keV ($Z \approx 50$) so that, with care, we can conclude that the X-ray absorption at energies above 40 keV in 10–50 μm sized crystals will be small or negligible.

2.4. Many-beam diffraction

One problem which arises in high-energy X-ray diffraction stems from the fact that the limiting sphere for Bragg reflection becomes large; many-beam simultaneous reflection is the norm and must be taken into account (Chang, 1984). In the energy range up to 100 keV the situation is not as complicated as in the electron case, because there is still a wavelength ratio of at least ten between the two probes.

2.5. Experimental feasibility

Equations (5) show that we require $A < 0.8$, corresponding to $t < 0.2\Delta_0$ in order to work in the regime where both kinematical and dynamical theories converge. Again, for Ag $K\alpha_1$ radiation and for silicon, quartz and germanium Table 1 shows typical values (from Pinsker, 1978, Table 3.1).

These results can be extrapolated to higher energies using the scaling factors given in (4), which indicate that the maximum crystal thickness may be around 10 μm or larger at energies above 22 keV. Absorption is also negligible. Since the integrated intensity is proportional to the sample volume in this diffraction regime, the earlier results which show intensities of around 1 s^{-1} from $1\text{ }\mu\text{m}^3$ samples from existing storage rings (Rieck & Schulz, 1991) allow us to predict one thousand times higher intensities from the same sources for $1000\text{ }\mu\text{m}^3$ samples and much more intensity with focused beam-lines. In this case, unlike the microcrystal situation, the signal-to-noise ratio will be significantly improved in proportion to the sample volume.

3. Concluding remarks

Single crystals in the size range 10–50 μm diameter examined at energies around 20–100 keV or higher will diffract very high intensities from available third-generation synchrotron radiation sources; they will have no extinction, primary or secondary, no significant

Table 1. Typical Bragg and Δ_0 values

Material	Bragg hkl	$0.2\Delta_0$ (μm)
Silicon	111	10.8
	220	9.3
	422	12.5
	333	18.6
	444	17.7
Quartz	1010	28.8
	1120	25.3
Germanium	111	4.7
	220	3.9
	422	5.2
	333	8.0
	444	7.4

absorption and the diffracted intensity will not be shape-dependent. Both dynamical theory and kinematical theory will be exact. The predicted intensity is sufficient for measurements to a statistical accuracy of 0.1% and the formulae for the integrated reflection power in terms of the charge density should be of comparable precision.

References

- ALKIRE, R. W. & YELON, Y. B. (1981). *J. Appl. Cryst.* **14**, 362–369.
 ALKIRE, R. W., YELON, Y. B. & SCHNEIDER, J. R. (1982). *Phys. Rev. B*, **26**, 3097–3104.
 CHANG, S.-L. (1984). *Multiple Diffraction of X-rays in Crystals*. Berlin: Springer-Verlag.
 GRAF, H. A. & SCHNEIDER, J. R. (1986). *Phys. Rev. B*, **34**, 8629–8638.
 FREUND, A. K. (1973). Dr rer nat thesis. München Univ., Germany, and ILL, Grenoble, France.
 FREUND, A. K. (1988) (Editor). *Applications of High Energy X-ray Scattering*. ESRF Workshop, 11–12 February, 1988.
 FREUND, A. K., HART, M. & SCHNEIDER, J. R. (1988). *Nucl. Instrum. Meth. A*, **266**, 247–251.
 HASTINGS, J. B., SIDMONS, D. P., BERMAN, L. E. & SCHNEIDER, J. R. (1989). *Rev. Sci. Instrum.* **60**, 2398–2401.
 PINSKER, Z. G. (1978). *Dynamical Scattering of X-rays in Crystals*. Berlin: Springer-Verlag.
 RIECK, W. & SCHULZ, H. (1991). *Handbook of Synchrotron Radiation*, edited by G. BROWN & D. E. MONCTON, Vol. 3, pp. 269–290. Amsterdam: Elsevier Science Publishers.
 RUTHERFORD, E. & ANDRADE, E. N. DA C. (1914). *Phil. Mag.* **6**, 263–273.
 SCHNEIDER, J. R. (1980). *Characterization of Crystal Growth Defects by X-ray Methods*, edited by B. K. TANNER & D. K. BOWEN, pp. 186–215. New York: Plenum Press.
 SCHNEIDER, J. R. (1981). *Nucl. Sin. Appl.* **1**, 227–276.
 WÖLFEL, E. (1975). *Theorie und Praxis der Röntgenstrukturanalyse*. Braunschweig: Vieweg.
 ZACHARIASEN, W. H. (1945). *Theory of X-ray Diffraction in Crystals*. New York: John Wiley.